Microsystem Technologies (2020) 26:2989–2996
https://doi.org/10.1007/s00542-020-04857-y

TECHNICAL PAPER

Influence of geometric parameters on the fluidic and mixing characteristics of T-shaped micromixer

Xuekuan Zhan[1] · Dalei Jing[1]

Received: 6 February 2020 / Accepted: 18 April 2020 / Published online: 26 April 2020
© Springer-Verlag GmbH Germany, part of Springer Nature 2020

Abstract
To understand the fluidic and mixing performances of passive micromixer, this paper numerically studies the influences of microchannel cross-sectional dimensions on the pressure drop and local mixing efficiency of T-shaped micromixer with three different cross-sectional shapes of rectangle, ellipse and isosceles triangle. Furthermore, a new dimensionless parameter is introduced to characterize the comprehensive fluidic and mixing performances of the main mixing channel and the whole T-shaped micromixer. It is found that both the fluidic and mixing performances of the T-shaped micromixer are sensitive to the cross-sectional dimensions of the microchannel. Among all the T-shaped micromixers with different microchannel cross-sectional shapes and different microchannel cross-sectional dimensions studied in this paper, the micromixer with elliptical-shaped microchannel having the dual axis length ratio of 0.5 is the optimal structure with the best comprehensive fluidic and mixing performances. The findings in present work are important for the design of the micromixer with desirable fluidic and mixing performances.

1 Introduction

As an important component unit of microfluidic system, micromixer has been widely used in various fields, such as medical testing, biochemical analysis, drug mixing and so on (Tsougeni et al. 2016; Phillips Reid et al. 2016; Chen 2013; Fletcher et al. 2003). In these applications, the main function of the micromixer is to achieve a thorough and rapid mixing of multiple samples. For example, in the microreactor, the micromixer can keep the effective mixing of the reagents and assure the occurrence of the chemical reaction (Chen 2013; Fletcher et al. 2003). Based on different energy source to achieve the mixing, the micromixer can be divided into two different classes, the passive micromixer and the active micromixer. Because of its compactness, low cost, easy integration, not easy to destroy the test liquid and other advantages, passive micromixer has been widely studied. However, for the passive micromixer, because its characterize size is small, the fluid flow within the mixing channel is mainly in laminar state and the main mixing mechanism is diffusion, thus, the mixing efficiency of passive micromixer is relatively limited. Thus, the mixing performance analysis and the mixing efficiency improvement of the passive micromixer has inspired wide scientific interests (Morteza et al. 2020; Haghighinia and Movahedirad 2019; Su et al. 2019; Mubashshir Ahmad and Wang 2008; Chen and Li 2016; Chen et al. 2017; Liu et al. 2012; Veldurthi et al. 2019; Lee et al. 2016; Cai et al. 2017; Jeon and Shin 2009). For example, Mubashshir Ahmad and Wang (2008) studied the mixing performance of 3D serpentine microchannel and found that the serpentine channel had better mixing performance than the straight channel. Chen and Li (2016), Chen et al. (2017) performed the structural topology optimization of waveform and serpentine channel of passive micromixer, and found that by changing the shape of microchannel, the chaotic convection and molecular diffusion were enhanced, resulting in better mixing performance. Jeon and Shin (2009) carried out studies on the effects of various microchannel obstructions on the mixing performance of the micromixer and found that zig-zag microchannels showed superior mixing compared to the other geometries.

Although comprehensive studies have been performed to understand the mixing performances of the passive micromixer, the fundamental mechanisms of micromixers

✉ Dalei Jing
jingdalei_hit@126.com

[1] School of Mechanical Engineering, University of Shanghai for Science and Technology, Shanghai 200093, People's Republic of China

still need further studies to design micromixer with optimal fluidic and mixing performances. One of the important reasons is that the fluidic resistance or pressure drop in the process of fluid mixing within the microchannel of the mixer is pretty high according to Poiseuille's law, since the characteristic size of micromixers is very small (Jing et al. 2020; Jing and Yi 2019; Shah and London 1978; Kandlikar et al. 2006). Therefore, it is necessary to reduce the energy consumption as much as possible on the basis of ensuring the mixing efficiency.

Therefore, this paper will carry out fundamental research on the influences of microchannel cross-sectional dimensions on the pressure drop, mixing efficiency and their combination of T-shaped micromixer with different microchannel cross-section shapes. The main aim of the present work is to understand the influences of microchannel geometric parameters on the comprehensive fluidic and mixing performances of the passive micromixer and further guide the optimization design of the passive micromixer with optimal fluidic and mixing performances.

2 Description of T-shaped micromixer

In present work, the T-shaped micromixers with different microchannel cross-sectional shapes of rectangle, ellipse and isosceles triangle shown in Fig. 1 are chosen to investigate the influences of microchannel cross-sectional geometric parameters on the fluidic and mixing characteristics of the micromixer. The cross-sectional geometries of the inlet microchannels and the main mixing microchannel of each micromixer are kept uniform. The total length of the inlet channels is set to be L_1 = 1300 μm and the length of the main mixing channel is L = 4000 μm. The width to height ratio ($\alpha = w/v$) of rectangular microchannel, the dual axis length ratio ($\beta = a/b$) of elliptical microchannnel and the base-to-height ratio ($\gamma = d/h$) of the isosceles triangular microchannel are

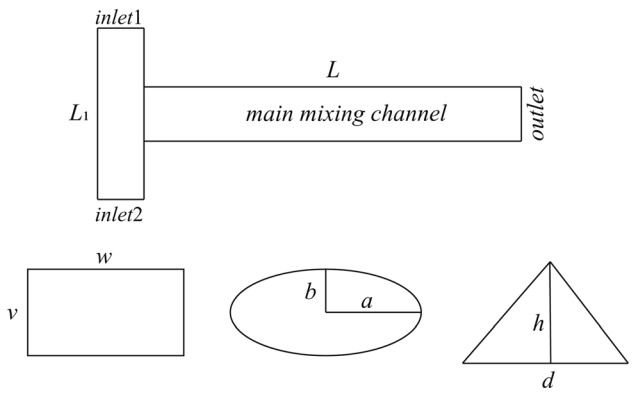

Fig. 1 Schematic diagram of T-shaped micromixer and the relevant microchannel cross-sectional shapes

adjusted under the size constraint of constant total channel volume of 4.77×10^8 μm^3 to investigate the influences of cross-sectional dimensions on the fluidic and mixing performances. Here, the directions of w, a and h of the main mixing channel are parallel to the axis direction of the inlet microchannel of the T-shaped micromixer. The specific cross-sectional dimensions of the T-shaped micromixer with different dimensions and configurations are shown in Tables 1, 2 and 3.

3 Numerical methodology

3.1 Governing equations and boundary conditions

In this study for evaluation of the fluidic and mixing performances of the T-shaped micromixer, all proposed designs are simulated by solving the following governing equations under the assumptions of incompressible Newtonian laminar flow in the microchannels.

The continuity equation and momentum equation for the fluid flow:

$$\nabla \cdot u = 0 \tag{1}$$

$$\rho(u \cdot \nabla u) = -\nabla p + (\mu \nabla u) \tag{2}$$

where u is the fluid velocity, ρ is the fluid density, μ is the dynamic viscosity of the liquid, and p is the pressure.

The convective diffusion equation for the mixing concentration calculation,

$$\frac{\partial c}{\partial t} + \nabla \cdot (-D\nabla c) = -u \cdot \nabla c \tag{3}$$

where c is the concentration, and D is the diffusion coefficient.

To perform the numerical studies, deionized water is chosen as the working liquid and its dynamic viscous, density and diffusion coefficient value used in the simulation setup were 0.001 Pa s, 1000 kg/m^3 and 1×10^{-10}m^2/s respectively.The initial conditions used are uniform velocity of 1×10^{-4} m/s at the inlets of micromixer and zero pressure at the outlet. No-slip velocity boundary condition is imposed at all the walls of the micromixer. The concentration values at inlet 1 and inlet 2 are given by 0 and 1 mol/m^3 respectively to display the mixing variation.

By solving the above governing equations using COMSOL, the velocity field, the pressure distribution and the concentration distribution can be obtained within the micromixer. Then, the following parameters are introduced to characterize the fluidic and mixing performances of the micromixer.

Table 1 Microchannel geometric dimensions of T-shaped micromixer with rectangular cross-sectional shape

$\alpha = w/v$	0.25	0.32	0.44	0.56	0.69	0.84	1	1.17	1.36	1.78
w (μm)	150	175	200	225	250	275	300	325	350	400
v (μm)	600	514.28	450	400	360	327.27	300	276.92	257	225

Table 2 Microchannel geometric dimensions of T-shaped micromixer with elliptical cross-sectional shape

$\beta = a/b$	0.225	0.283	0.35	0.64	1	1.4	2.193	3.141	5.587	8.772
a (μm)	80	90	100	135	169.25	200	250	300	400	500
b (μm)	356	318.3	286	212.22	169.25	143	114	95.5	71.6	57

Table 3 Microchannel geometric dimensions of T-shaped micromixer with isosceles triangular cross-sectional shape

$\gamma = d/h$	0.5	0.68	0.89	1	1.08	1.125	1.18	1.25	1.39	1.68
d (μm)	300	350	400	425	440	450	460	475	500	600
h (μm)	600	514.3	450	423.53	409.1	400	391.3	378.98	360	327.3

The dimensionless pressure drop Δp^* to characterize the fluidic performance of the T-shaped micromixer,

$$\Delta p^* = \frac{\Delta p}{\rho u_{ref}^2} = \frac{p_{in} - p_{out}}{\rho u_{ref}^2} \tag{4}$$

where u_{ref} is the reference fluid velocity, which is equal to the inlet velocity, and Δp is the pressure drop between the inlets and outlet of the micromixer. Under the parametric setup of present work, the inlet velocity is fixed, thus, the smaller the dimensionless pressure drop is, the less energy consumption is required for mixing and the better the fluidic performance of the micromixer is.

The dimensionless local mixing efficiency M to characterize the mixing performance of the T-shaped micromixer (Chen and Li 2016; Chen et al. 2017; Chen and Zhang 2018),

$$M = 1 - \sqrt{\frac{1}{N}\sum_{i=1}^{N}\left(\frac{c_i - \bar{c}}{\bar{c}}\right)^2} \tag{5}$$

where, c_i is the concentration of sampling point at any cross-section of the mixing channel, $\bar{c}$ is the reference concentration for the fully mixed case and $\bar{c} = 0.5$ in present work, and N is the total number of sampling points used to calculate the local mixing efficiency. Here, the local mixing efficiency reflects the local mixing uniformity and degree of mixing at any cross-section of the mixing channel, and it ranges from 0 (zero mixing) to 1 (full mixed).

Furthermore, in order to characterize the comprehensive fluidic and mixing performances of the micromixer, the following dimensionless parameter η is introduced to characterize the comprehensive fluidic and mixing performance of the micromixer,

$$\eta = \frac{M_{out}}{\Delta p^*} \tag{6}$$

where M_{out} is the outlet mixing efficiency that is an index of the mixing performance. This comprehensive parameter $M_{out}/\Delta p^*$ represents the outlet mixing efficiency per unit dimensionless pressure drop. When the dimensionless pressure drop is given, the greater the comprehensive parameter is, the larger outlet mixing efficiency is, that is, the more uniform the mixing is and the better the mixing performance is. In other word, with certain mixing efficiency, the greater the comprehensive parameter is, the smaller the dimensionless pressure drop is and the smaller the required energy consumption is. Thus, the micromixer with a larger $M_{out}/\Delta p^*$ has better comprehensive fluidic and mixing performance.

3.2 Grid independent and data validation

In order to ensure the correctness of the numerical simulation and the accuracy of mesh generation, it is necessary to test the dependence of the numerical results on the grid size to prevent errors in the simulation results due to unreasonable mesh generation. Tetrahedral meshes are used in each simulation. The following is an example of the mesh-independence test based on previous method (Jing and He 2019). For a T-shaped micromixer with rectangular microchannel of w/v= 1, six groups of tetrahedral meshes of different numbers were selected to mesh the micromixer. The pressure drop, outlet concentration, and the relevant errors for pressure drop and outlet concentration are

calculated, as shown in Table 4. It can be found that when the mesh number is 41,886, the relevant errors for pressure drop and outlet concentration are 1.28×10^{-4} and -1.57×10^{-2}, which are good enough to keep the accuracy of the numerical results, thus, this mesh is used. The same grid independence test is carried out for each simulation to keep the accuracy of the numerical results.

In addition to the grid independence test, the mixing efficiency obtained by using the present numerical method in this paper were further compared with the numerical and experimental results of T-shaped micromixer in Ref. Rismanian et al. (2019) for the data validation, as shown in Fig. 2. All the simulation parametric setup for the data validation from Ref. (Rismanian et al. 2019) is as follows. The channel cross-sectional shape of the T-shaped mixer is rectangle. The total length of the inlet channels is $L_1 = 2.2$ mm and the length of the outlet channel is $L = 33$ mm. The microchannel width (w) and height (v) are 0.2 mm and 0.3 mm. From Fig. 2, it can be found that the present numerical results are well consistent with the existing studies with high accuracy. This shows that the numerical model in present work is feasible.

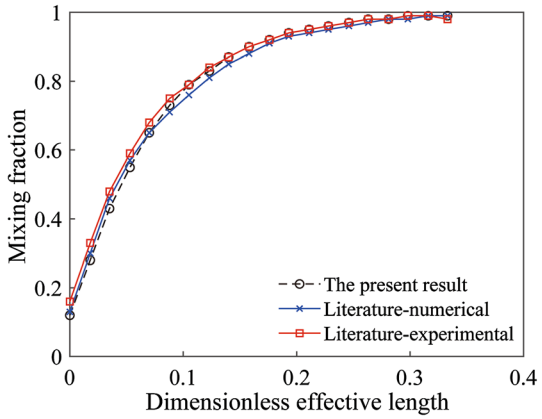

Fig. 2 Comparison of the mixing efficiency obtained from present work and numerical and experimental results in literature (Rismanian et al. 2019)

4 Results and discussion

4.1 Pressure drop

Based on the proposed numerical method, Fig. 3 gives the effects of the microchannel cross-sectional geometric parameters on the dimensionless pressure drop of the T-shaped micromixer with rectangular-, elliptical- and triangular-shaped microchannels. It can be found from Fig. 3 that the dimensionless pressure drop first decreases and then increases with the increasing width to height ratio for rectangular microchannel, the increasing dual axis length ratio for elliptical microchannnel and the increasing base-to-height ratio for isosceles triangular microchannel. This is consistent with the previous studies (Jing and He 2019; Kwang et al. 2012; Gunnasegaran et al. 2010; Mortensen et al. 2005), and can be easily explained by the Poiseuille's law (Shah and London 1978; Kandlikar et al. 2006). Based on the Poiseuille's law, the pressure drop of laminar flow within a microchannel is inversely proportional to the fourth power of microchannel hydraulic diameter when the flowrate of the flow is fixed. Thus, the microchannel with largest hydraulic diameter has a smallest pressure drop. In present work, the cross-sectional area of each T-shaped micromixer with different channel cross-sectional shape and channel cross-sectional dimension is same, then by calculating the microchannel hydraulic diameter, it is easy to find that for the three groups of micromixers with different channel cross-sectional shapes, the micromixers with square-shaped microchannel ($w/v = 1$), circle-shaped microchanenl ($a/b = 1$) and the equilateral trianglular-shaped microchannel ($d/h = 2/\sqrt{3}$) have the largest hydraulic diameters, thus, their pressure drop is smallest, as shown in Fig. 3.

4.2 Local mixing efficiency

To display the concentration variation within the micromixer, Fig. 4 gives the concentration profiles within the T-shaped micromixer with square, circle and equilateral triangle channel cross-sections. From Fig. 4, it can be found that the mixing starts when the two liquids with different concentration denoted as blue and red colors enters the mixing channel, and the degree of mixing increases with the increase of mixing length due to the

Table 4 Example of grid independence test

Test number i	Mesh number	Δp [Pa]	$(\Delta p^{i+1} - \Delta p^i)/\Delta p^i$	C_{outlet}	$(c^{i+1}_{outlet} - c^i_{outlet})/c^i_{outlet}$
0	1040	0.2737958	–	0.3527	–
1	2125	0.2748886	3.99×10^{-3}	0.3255	-7.7×10^{-2}
2	6174	0.2754411	2.01×10^{-3}	0.3008	-7.59×10^{-2}
3	12879	0.2753945	-1.69×10^{-4}	0.2929	-2.63×10^{-2}
4	41886	0.2754297	1.28×10^{-4}	0.2883	-1.57×10^{-2}
5	174972	0.2756231	7.02×10^{-4}	0.2875	-2.775×10^{-3}

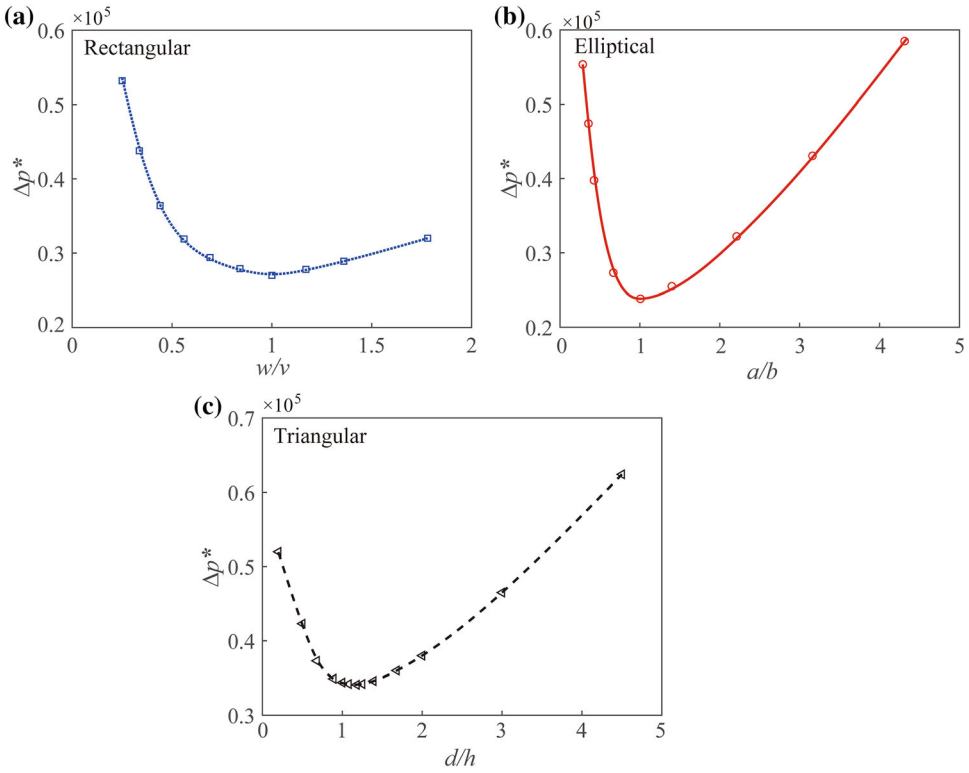

Fig. 3 Dimensionless pressure drop of T-shaped micromixers with rectangular, elliptical and triangular cross-sectional shape

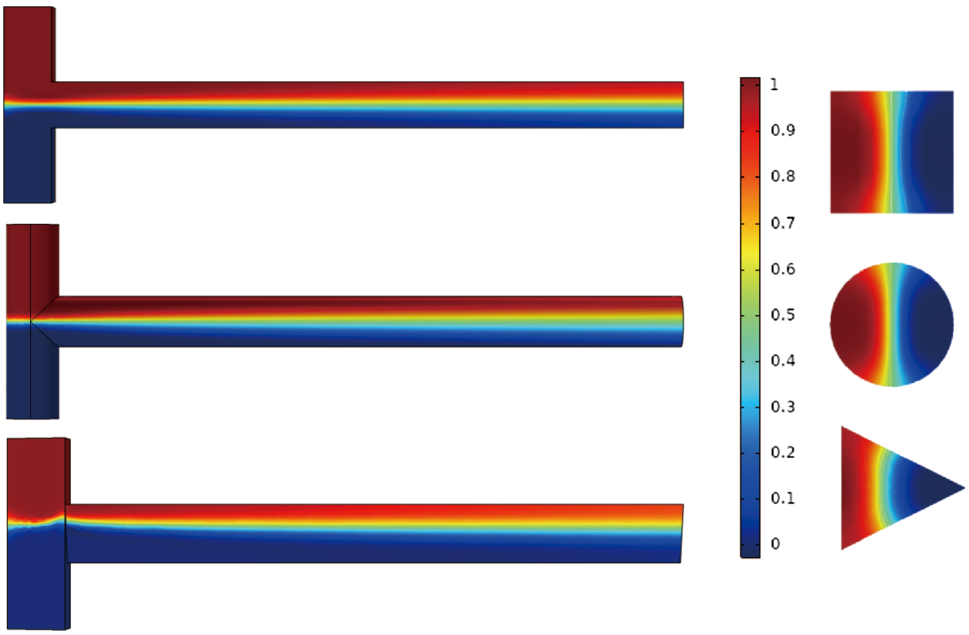

Fig. 4 Concentration profiles of T-shaped micromixer with square, circle and equilateral triangle microchannel cross-section

contact diffusion time and the molecular diffusion distance of the two liquids increase with the increase of the mixing length.

To further quantify the effects of the microchannel cross-sectional geometric parameters on the mixing performance, Fig. 5 gives the effects of the microchannel cross-sectional geometric parameters on the local mixing efficiency along the length direction of the mixing channel with rectangular-, elliptical- and triangular-shaped microchannels. It can be found that the mixing efficiency increases gradually with the decreasing width to height ratio for rectangular microchannel, the decreasing dual axis length ratio for elliptical microchannnel, and the increasing base-to-height ratio for isosceles triangular microchannel.

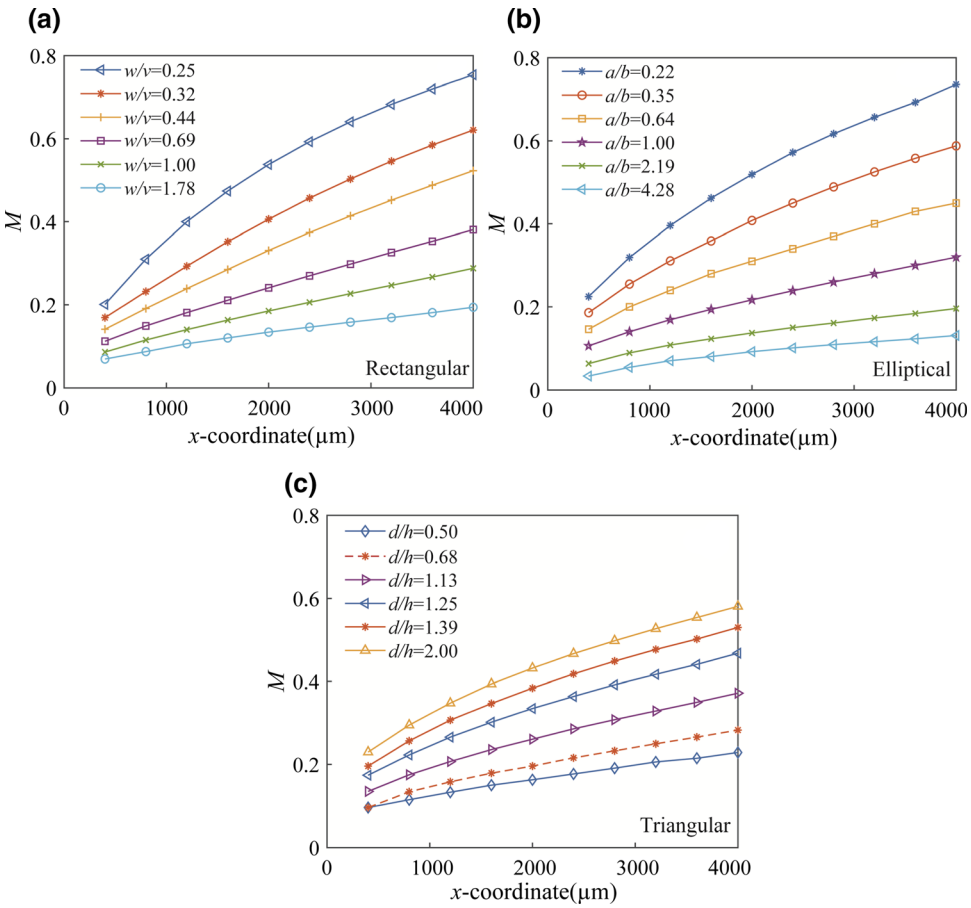

Fig. 5 Local mixing efficiency of T-shaped micromixer with rectangular, elliptical and triangular-shaped channel

This is consistent with the conclusions of previous studies (Su et al. 2019; Chen and Li 2016; Chen et al. 2017). The main reason for these results is as follows. For the mixing within a passive micromixer, the main mixing mechanism is free diffusion, and the degree of mixing is related to the $t = x^2/D$ (where t is the diffusion time, x is the distance to mixing and D is the diffusion coefficient). The smaller the distance to mixing is, the larger the mixing efficiency is. In present work, with the decreasing width to height ratio of the rectangular-shaped microchannel, the decreasing dual axis length ratio of the elliptical-shaped microchannnel, and the increasing base-to-height ratio of the isosceles triangular-shaped microchannel, the effective distance to mixing becomes smaller, thus, the diffusion time to mix becomes shorter and the corresponding mixing efficiency is larger, as shown in Fig. 5.

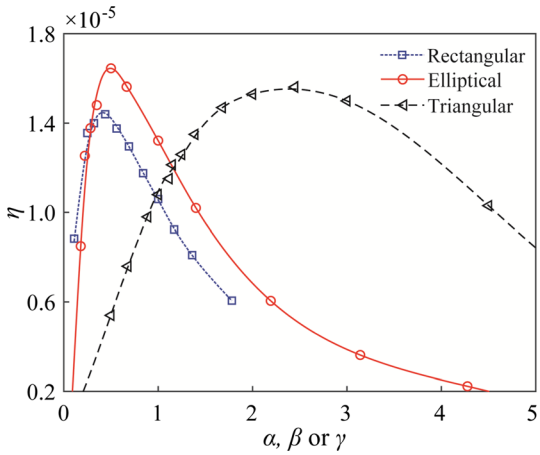

Fig. 6 Comprehensive performance of T-shaped micromixer with rectangular, elliptical and triangular microchannel cross-section

4.3 Comprehensive fluidic and mixing performance

Considering the mixing occurs in the main mixing channel, thus, Fig. 6 gives the comprehensive fluidic and mixing performance η of the main mixing channel with different cross-sectional shapes and dimensions. It can be found that the comprehensive performance parameter η first increases and then decreases with the increasing width to height ratio for rectangular microchannel, the increasing dual axis length ratio for elliptical microchannnel and the increasing base-to-height ratio for isosceles triangular microchannel. This means that there is an optimal cross-sectional dimension at where the comprehensive fluidic and mixing

performance of the main mixing channel is best. It can be found that when w/v = 0.4, a/b = 0.5 and d/h = 2.5, the η is largest for the rectangular-, elliptical- and triangular-shaped mixing microchannel.

In order to further analyze the comprehensive fluidic and mixing performance of the entire micromixer, Fig. 7 gives the comprehensive fluidic and mixing performance of the whole T-shaped micromixer with different cross-sectional shapes and dimensions. Being similar to the comprehensive performance parameter η of the main mixing channel, it can be observed that the comprehensive performance parameter η of the whole micromixer also displays the trend of first increases and then decreases with the increasing width to height ratio for rectangular microchannel, the increasing dual axis length ratio for elliptical microchannnel and the increasing base-to-height ratio for isosceles triangular microchannel. Further comparing the comprehensive performance parameter η of the T-shaped micromixer with different microchannel cross-sectional shapes, it can be found that when the dual axis length ratio a/b of the micromixer with elliptical-shaped channel is 0.5, it has the largest η and the best comprehensive fluidic and mixing performance.

5 Conclusions

This paper numerically studies the influences of microchannel cross-sectional dimensions on the fluidic and mixing performances of T-shaped micromixer with three different cross-sectional shapes of rectangle, ellipse and isosceles triangle under the size constraint of constant total channel volume. It is found that the dimensionless pressure drop first decreases and then increases with the increasing width to height ratio for the micromixer of rectangular microchannel, the increasing dual axis length ratio for the micromixer of elliptical microchannnel and the increasing base-to-height ratio for the micromixer of isosceles triangular microchannel. However, the mixing efficiency increases gradually with the decreasing width to height ratio for the micromixer of rectangular microchannel and the decreasing dual axis length ratio for the micromixer of elliptical microchannnel and the increasing base-to-height ratio for the micromixer of isosceles triangular microchannel. Furthermore, the comprehensive fluidic and mixing performances of both the main mixing channel and the whole T-shaped microchannel first increases and then decreases with the increasing width to height ratio for the micromixer of rectangular microchannel, the dual axis length ratio for the micromixer of elliptical microchannnel and base-to-height ratio for the micromixer of isosceles triangular microchannel. The T-shaped micromixer with elliptical microchannel cross-section having the dual axis length ratio of a/b = 0.5 is the optimal micromixer with the best fluidic and mixing performances.

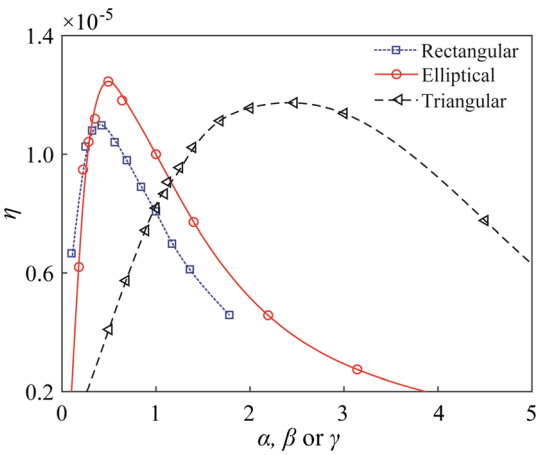

Fig. 7 Comprehensive performance of T-shaped micromixer with rectangular, elliptical and triangular-shaped microchannel

Acknowledgement The authors gratefully acknowledge the financial support of the National Natural Science Foundation of China (No. 51505292).

Compliance with ethical standards

Conflict of interest The authors have no conflict of interest.

References

Cai G, Xue L, Zhang H, Lin J (2017) A review on micromixers. Micromachines 8(9):274

Chen P (2013) An evaluation of a real-time passive micromixer to the performance of a continuous flow type microfluidic reactor. BioChip J 7(3):227–233

Chen X, Li T (2016) A novel design for passive misscromixers based on topology optimization method. Biomed Microdevices 18(4):57

Chen X, Zhang S (2018) 3D micromixers based on Koch fractal principle. Microsyst Technol 24:2627–2636

Chen X, Li T, Hu Z (2017) A novel research on serpentine microchannels of passive micromixers. Microsyst Technol 23:2649–2656

Fletcher PDI, Haswell SJ, Zhang X (2003) Monitoring of chemical reactions within microreactors using an inverted Raman microscopic spectrometer. Electrophorisis 24:3239–3245

Gunnasegaran P, Mohammed H, Shuaib N, Saidur R (2010) The effect of geometrical parameters on heat transfer characteristics of microchannels heat sink with different shapes. Int Commun Heat Mass Transf 37(8):1078–1086

Haghighinia A, Movahedirad S (2019) Mass transfer in a novel passive micro-mixer: flow tortuosity effects. Anal Chim Acta 1098:75–85

Jeon W, Shin C (2009) Design and simulation of passive mixing in microfluidic systems with geometric variations. Chem Eng J 152:575–582

Jing D, He L (2019) Numerical studies on the hydraulic and thermal performances of microchannels with different cross-sectional shapes. Int J Heat Mass Transf 143:118604

Jing D, Yi S (2019) Electroosmotic flow in treelike branching microchannel network. Fractals 27(6):1950095

Jing D, Song J, Sui Y (2020) Hydraulic and thermal performances of laminar flow in fractal treelike branching microchannel network with wall velocity slip. Fractals. https://doi.org/10.1142/S0218348X2050022X

Kandlikar SG, Garimella S, Li DQ, Colin S, King MR (2006) Heat transfer and fluid flow in minichannels and microchannels. Elsevier, Oxford

Kwang W, Lee K, Furlani Edward P (2012) Design of pressure-driven microfluidic networks using electric circuit analogy. Lab Chip 12(3):515–545

Lee C, Wang W, Liu Ch, Fu L (2016) Passive mixers in microfluidic systems: a review. Chem Eng J 288:146–160

Liu Z, Lu Y, Wang J, Luo G (2012) Mixing characterization and scaling-up analysis of asymmetrical T-shaped micromixer: experiment and CFD simulation. Chem Eng J 181–182:597–606

Mortensen N, Okkels F, Bruus H (2005) Reexamination of Hagen-Poiseuille flow: shape dependence of the hydraulic resistance in microchannels. Phys Rev E 71:057301

Morteza B, Mohsen Nazemi A, Azam U (2020) Active and passive micromixers: a comprehensive review. Chem Eng Process Process Intensif 147:107771

Mubashshir Ahmad A, Wang Y (2008) Parametric study on mixing of two fluids in a three-dimensional serpentine microchannel. Chem Eng J 146(3):439–448

Phillips Reid H, Jain R, Browning Y, Shah R, Kauffman P, Dinh D, Lutz Barry R (2016) Flow control using audio tones in resonant microfluidic networks: towards cell-phone controlled lab-on-a-chip devices. Lab Chip 16(17):3260–3267

Rismanian M, Mohammad S, Navid K (2019) A new non-dimensional parameter to obtain the minimum mixing length in tree-like concentration gradient generators. Chem Eng Sci 195:120–126

Shah RK, London AL (1978) Laminar flow forced convection in ducts. Academic Press, Cambridge

Su T, Cheng K, Wang J, Xu Zh, Dai W (2019) A fast design method for passive micromixer with angled bend. Microsyst Technol 25(11):4391–4397

Tsougeni K, Papadakis G, Gianneli M, Grammoustianou A, Constantoudis V, Dupuy B, Petrou PS, Kakabakos SE, Tserepi A, Gizeli E, Gogolides E (2016) Plasma nanotextured polymeric lab-on-a-chip for highly efficient bacteria capture and lysis. Lab Chip 16(1):122–131

Veldurthi N, Bodas D, Chandel S, Tejashree B (2019) Geometrically similar rectangular passive micromixers and the scaling validity on mixing efficiency and pressure drops. J Mech Eng 69(1):69–84

Publisher's Note Springer Nature remains neutral with regard to jurisdictional claims in published maps and institutional affiliations.